

Tracking a mobile robot in a UWB-sensor grid

JORGE A. ORTEGA-CONTRERAS, YURIY S. SHMALIY, JOSE A. ANDRADE-LUCIO,
MIGUEL VAZQUEZ-OLGUIN, ELI G. PALE-RAMON, KAREN URIBE-MURCIA

Dept. of Electronics Engineering, Universidad de Guanajuato Salamanca, MEXICO

Abstract: This work presents the development of a tracking system for a three-wheeled omnidirectional mobile robot. This kind of robot can perform rotation and translation in any pose. The arc-length segment described by the omni-wheels controls the trajectory of the robot. We present a simplified kinematic model in state-space. The observation system is based on an UltraWide Band ranging sensor. Finally made the state estimation using some classic positioning algorithms and compare the results against Finite Impulse Response Filter state estimators.

Keywords: Kalman Filter, EOFIR Filter, State Estimation, UWB sensor

Received: May 29, 2021. Revised: June 9, 2022. Accepted: July 12, 2022. Published: August 2, 2022.

1. Introduction

Actually, wheeled mobile robots(WMR) have applications in many fields like personal care [1], health [2], and manufacturing process [3]. Omnidirectional mobile robots (OMR) are vehicles are attracting more attention because of his capability to reach any posture independently of his orientation. Nowadays, mobile robots seems to be a new trend in Industry 4.0 [4], the control [5], motion analysis [6] and path planning [7] are common challenges in the design of a robot, but with the need of cooperative robots the location tasks difficulty is increasing [8]. The robot needs data to perform a task. Using several UltraWide band (UWB) ranging sensors, we estimate the localization of the OMR . UWB technology can achieve precise localization [9] and is a great option to implement sensor networks due to its power consumption efficiency and robustness in harsh environments. Here, we discuss the case of the three wheeled omnidirectional robot(TWOR) moving along a UWB sensor network [10]. In [11], [12] the authors present a model for UWB range measurement. Classic methods of state estimation are in [13]–[16]. Some troubles in UWB ranging are covered in [17], [18] were the authors discussed the mitigation of error when the sensors are out of sight.

Identify applicable funding agency here. If none, delete this.

2. Kinematic Analysis of the Mobile Robot

In this section, we show the geometric modeling of TWOR. We develop the model in discrete-time and, to apply the estimation algorithms, we take the kinematic model into its state-space representation. A TWOR is pictured in Fig. 1. Because of its kinematic constraints, this kind of robot has the same number of actuation and degrees of freedom. Therefore, they can perform translational and rotational motions at the same time [19].



Fig. 1. Festo Robotino Mobile Robotic Development Platform

2.1. Description of the Mobile Robot

We equipped the TWOR with three omnidirectional wheels (OMW) [20]. They comprise a set of bottom-rollers arranged around a rotation axis. In our case, the axes of the rollers and the wheel are perpendicular. In figure 2, we sketch an

OMW with perpendicular rollers. The axes of rotation of the omni-wheel axis are independent of each other. We consider that the actuation signal u_n represent the displacement of the wheel. An omni-directional drive system requires at least three points of intersection between the axes of the bottom-rollers to satisfy the full-rank condition for the Jacobian of the wheel orientation matrix [7].

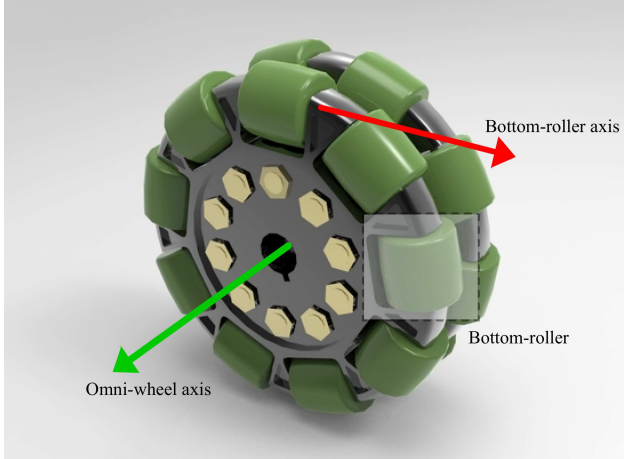


Fig. 2. Omni-wheel 3D model

For the topology of the robot, we use rotational symmetry configuration [19]. In order to balance the vertical reaction in the wheels and, in consequence, get similar longitudinal friction forces. The TWOR used in our experiment have a diameter of 60cm and use omnidirectional wheels with radius of 5cm. Depending on the dynamic constraints, a mobile wheeled robot can control each DOF independently.

2.2. Kinematics of the Transition State Function

A kinematic diagram of a three-wheeled omnidirectional robot (TWOR) with perpendicular rollers is shown in Fig. 3. We use the following notations and symbols to describe the system model

- World frame coordinates
 - x_n, y_n Position of the robot
 - x, y World coordinate system
 - Φ_n Orientation of the local frame referred to the world system
- Local frame coordinates
 - p_n Total displacement of the robot
 - φ_n Angle of the displacement vector referred to the local frame
 - u_i Arc-length step of the wheels
 - x_L, y_L Local coordinate system
- Model constants
 - R Radius of the robot

The robot is driven by the displacement of its wheels. Assuming a pure-roll condition, the displacement Δu_j can be found by:

$$\Delta u_j = \left\| \text{proj}_{\mathbf{u}_j} \mathbf{u}_{x_L} \right\| + \left\| \text{proj}_{\mathbf{u}_j} \mathbf{u}_{y_L} \right\| + \Delta \varphi * R, \quad (1)$$

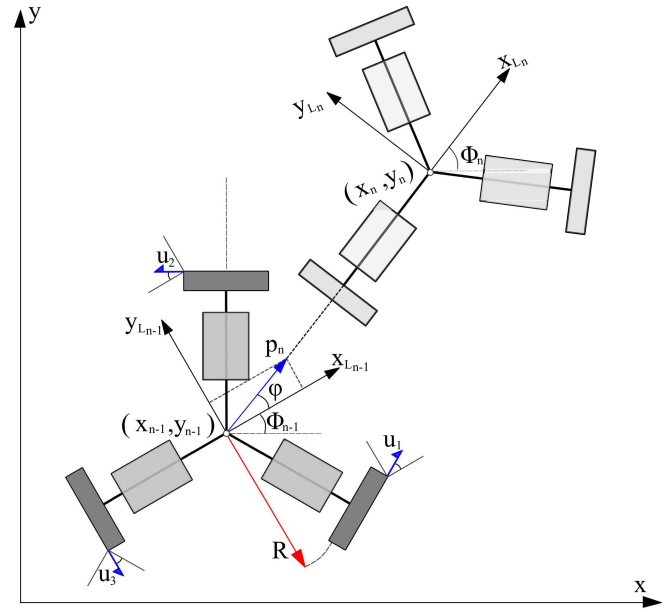


Fig. 3. Kinematic diagram of TWOR

From (1), the robot kinematics in state-space representation is as follows:

$$\begin{bmatrix} \Delta u_1 \\ \Delta u_2 \\ \Delta u_3 \end{bmatrix} = \begin{bmatrix} \cos \pi/6 & \sin \pi/6 & R \\ -\cos \pi/6 & \sin \pi/6 & R \\ 0 & -1 & R \end{bmatrix} \begin{bmatrix} \Delta u_{x_L} \\ \Delta u_{y_L} \\ \Delta \varphi \end{bmatrix}, \quad (2)$$

$$\Delta U_i = \mathbf{A} \Delta U_L$$

Where ΔU_i is the displacements vector, ΔU_L is the robot position vector in the local frame, and \mathbf{A} is the system matrix. By inverting (2), we have

$$\Delta U_L = \mathbf{A}^{-1} \Delta U_i$$

$$\mathbf{A}^{-1} = \begin{bmatrix} \sqrt{3}/3 & -\sqrt{3}/3 & 0 \\ 1/3 & 1/3 & -2/3 \\ 1/3R & 1/3R & 1/3R \end{bmatrix}. \quad (3)$$

And applying a rotation to transform into the world frame, we get

$$\Delta U = R(\Phi) U_L$$

$$\Delta U = R(\Phi) \mathbf{A}^{-1} U_i \quad (4)$$

Then, each coordinate can be written as:

$$\Delta u_x = \frac{\sqrt{3}}{3} \Delta u_{12} \cos(\Phi_{n-1}) - \frac{1}{3} \Delta u_{123} \sin(\Phi_{n-1}), \quad (5)$$

$$\Delta u_y = \frac{\sqrt{3}}{3} \Delta u_{12} \sin(\Phi_{n-1}) + \frac{1}{3} \Delta u_{123} \cos(\Phi_{n-1}), \quad (6)$$

$$\Delta \varphi = \frac{1}{3R} (\Delta u_1 + \Delta u_2 + \Delta u_3), \quad (7)$$

Where $\Delta u_{12} = \Delta u_1 - \Delta u_2$ and $\Delta u_{123} = \Delta u_1 + \Delta u_2 - 2\Delta u_3$. We can measure the real displacement of the wheel using incremental encoders, therefore the quantities $\Delta u_1, \Delta u_2$, and Δu_3 are known. The model can be simplified by considering

p_n and $\Delta\varphi$ as exogenous variables. Doing some trigonometric transformations in (5-6) we can show that:

$$p_n = \frac{1}{3} \sqrt{3\Delta u_{12}^2 + \Delta u_{123}^2}, \quad (8)$$

$$\varphi_n = \Delta\varphi_n + \Phi_{n-1}, \quad (9)$$

By introducing the state vector $x_n = [x_{1n} \ x_{2n} \ x_{3n}]^T$ of the global coordinates, with the components

$$\begin{aligned} x_{1n} &= x_{1n-1} + p_n \cos(x_{3n-1} + \Delta\varphi_n), \\ x_{2n} &= x_{2n-1} + p_n \sin(x_{3n-1} + \Delta\varphi_n), \\ x_{3n} &= x_{3n-1} + \Delta\varphi_n, \end{aligned} \quad (10)$$

We can write the nonlinear state equation as:

$$x_n = \mathbf{f}_n(x_{n-1}, u_n, w_n), \quad (11)$$

where $w_n \sim \mathcal{N}(0, Q_n)$ is zero mean white Gaussian noise with the covariance Q_n .

2.3. Observation Model

We will derive localization information in UWB based positioning system through different measurements like RSSI or ToF, we deploy our setup using the Decawave DW1000 transceiver with a bandwidth of 900MHz and IEEE 802.15.4a compliant. The distance between anchor and tags will be calculated using Asymmetric Double sided Two-way ranging (AltDS-TWR) [21], [22]. Basically, AltDS-TWR derive the range estimation based on the round-trip delay between two data bursts. This algorithm has the smallest error due to clock drift [23] even if the error increase with the distance, the order is less than 30cm for a clock-drift $xi < 3ppm$ and a $t_{reply} < 650\mu s$. We take the distance data from multiple DWM1000 modules configured as an anchor. We also assume the position of each anchor is fixed and known. An additional DWM1000 module configured as a tag is attached to the TWOR. The figure 4 shows the test environment used in the experimental evaluation. We can write the distance between k-anchor and tag as:

$$r_k = \sqrt{(x_k - x_{1n})^2 + (y_k - x_{2n})^2} \quad (12)$$

Where x_k, y_k are the position of the k-anchor. We assume there is no z-level changes and the transceiver modules (anchors-tag) are z-aligned. The radiation pattern (Fig. 4) in the horizontal plane is omnidirectional [10] if the transceivers are vertically oriented.

1) *Sources of error*: The ideal case appears when the transceivers are in line of sight (LOS), here the only source of error is systematic. Several factors as reflection and diffraction, will affect the measurements [24]. When the robot navigates in complex environments, it can be under a non-line of sight (NLOS) conditions or multi-path phenomena, which can affect the accuracy of the measurements. A deterministic model for UWB channel mode must be capable of describing LOS or NLOS conditions at the same time without a priori information. Due to the difficulties presented in real scenarios,

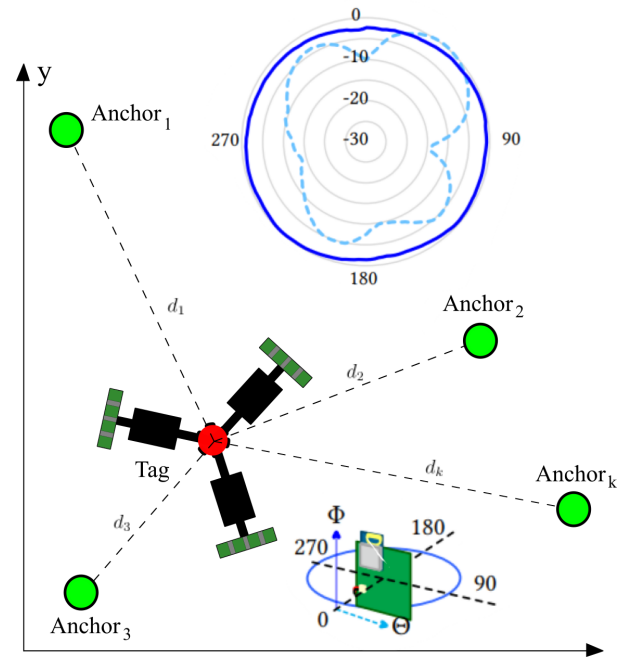


Fig. 4. Deploy of tag and anchors in the system

we propose a previous experimental test to find a model for signal attenuation in LOS conditions.

$$d_k = \sqrt{(a_k - \bar{x}_n)^T (a_k - \bar{x}_n) + \text{bias}(r_k) + v_k} \quad (13)$$

Where a_k is the X-Y coordinates vector of the tag, and \bar{x}_n is the first two elements of the x_n position vector. The vector v_n is the observation noise modelled as a random variable with white-Gaussian distribution, zero-mean and covariance Q_n . We can write the nonlinear observation model as:

$$d_n = \mathbf{g}_n(x_n, v_n) \quad (14)$$

3. Tracking Twor in Sensor Grid

In this section, we are going to compare classical position estimators, such as Least Squares, Extended Kalman against FIR Estimators, using a simple observation model and the bias-corrected model. We propose a covariance model to mitigate the error due to NLOS using a binary discrimination.

3.1. Characterization of Single Uwb Sensor in Los

Our characterization environment was an ideal scenario, with LOS connection between tag and anchor. In this condition, the measured signal corresponds to the distances between transceivers with some additive noise. The measurements succeed in an area of 5m x 8m with no obstacles between the transceivers. The walls can't induce multipath error, because the distance between the transceivers is small, compared with the distance of the multipath trajectory. With the DWM1000 modules vertically aligned and separated from the floor, at a distance of 1.5m, we are making ranging measurements. When the distance between transceivers is increasing, we get a bigger bias, as shown in figure 5 .

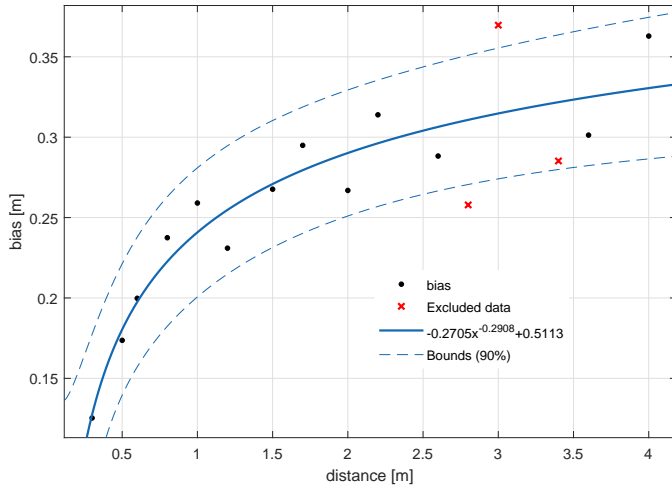


Fig. 5. Increase of the bias as a function of the distance

In LOS conditions, the destructive interference with ground reflected signal can cause attenuation, leading to the bias phenomena. To get an approximated model, we fit the bias to a polynomial function, the equation 13 is now:

$$r_k = \sqrt{(a_k - \bar{x}_n)^T (a_k - \bar{x}_n)} \quad (15)$$

$$d_k = r_k - 0.2705r_k^{-0.2908} + 0.5113 + v_k$$

We set the covariance of v_k as the mean of the experimental values, then $\sigma_v^2 = 0.0105$

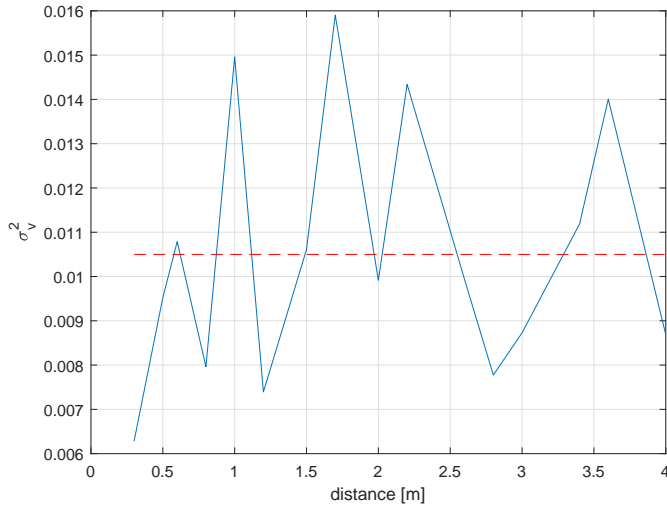


Fig. 6. Covariance of the measurements

Finally, the observation model must be capable of minimizing the influence of NLOS measurements in the estimation, thus we define a binary rule:

$$\sigma_{v,k}^2 = \begin{cases} 0.0105 & |r_k - H_n \hat{x}_n| < \epsilon \\ 100 & otherwise \end{cases} \quad (16)$$

With the restriction in Eq.16 the value of ϵ act as a threshold, when the k-measurement is far from the predicted distance,

we must suppose an outlier. And then, we set his covariance as a 'big' value. This will cause that the estimator has less confidence in the measurement. And then minimize their impact on the state estimation.

3.2. Tag Localization

When the robot navigates into a real scenario, without prior knowledge of the space configuration, it will require many static anchor nodes with a known position. We are going to compare to different approaches, non-probabilistic approach and stochastic algorithms.

1) *Least Squares Estimator*: A set of discrete measurements y_n are assumed to be a linear function of unknown parameters and some additive noise. Then, for the linear model $y_n = H_n x_n + v_n$ the solution \hat{x}_n that minimize the squared-error is given by:

$$\hat{x}_n = (H_n^T H_n)^{-1} H_n^T y_n \quad (17)$$

To get a linear model from the measurement, we rewrite the euclidian distance between node and anchor, then we get:

$$R = x^2 + y^2$$

$$\hat{x}_n = [x \quad y \quad R]^T$$

$$H_n = \begin{bmatrix} -2x_1 & -2y_1 & 1 \\ -2x_1 & -2y_1 & 1 \\ \vdots & \vdots & \vdots \\ -2x_n & -2y_n & 1 \end{bmatrix}$$

$$y_n = \begin{bmatrix} d_1^2 - x_1^2 - y_1^2 \\ d_2^2 - x_2^2 - y_2^2 \\ \vdots \\ d_n^2 - x_n^2 - y_n^2 \end{bmatrix}$$

2) *Extended Kalman Filter*: Consider the nonlinear system defined by equations 11,14. Assume we have an initial state x_0 with known mean and covariance. The noises w_n and v_n are temporally uncorrelated. In the initial step, we made a prediction of state using:

$$\hat{x}_n^- = f_n(\hat{x}_{n-1}, u_n, 0)$$

$$P_n^- = F_n P_{n-1} F_n^T + W_n Q_n W_n^T$$

The correction step is given by

$$K_n = P_n^- H_n^T (H_n P_n^- H_n^T + V_n R_n V_n^T)^{-1}$$

$$\hat{x}_n = \hat{x}_n^- + K_n (y_n - h(\hat{x}_n^-, 0))$$

$$P_n = (I - K_n H_n) P_n^-$$

Where F_n is the Jacobian of the system model evaluated in the previous estimation point \hat{x}_{n-1} and H_n is the Jacobian of the observation model evaluated in the predicted state \hat{x}_n^- . Q_n is the noise model covariance, and R_n is the measurement noise covariance. In our case, W_n and V_n are the identity matrix I .

3) Extended Optimal Finite Impulse Response Filter:

The EOFIR filter is the most general optimal FIR estimator (Algorithm 1). We compute optimal estimates using Kalman recursions. The estimation will be bounded and the EOFIR Filter is BIBO stable for stable systems. The EOFIR filter has better response in the presence of disturbance due to the length of the horizon $[m, k]$.

Algorithm 1: EOFIR Filtering Algorithm

Input: $y_k, \hat{x}_m, P_m, Q_k, R_k, N$

Output: \hat{x}_k

```

1 for  $k = 1, 2 \dots \text{do}$ 
2   if  $k > N - 1$  then
3      $m = k - N + 1$ 
4   else
5      $m = 0$ 
6   end
7   for  $l = m + 1 : k$  do
8      $\bar{x}_l^- = f_l(\bar{x}_{l-1})$ 
9      $P_l^- = F_l P_{l-1} F_l^T + Q_l$ 
10     $S_l = H_l P_l^- H_l^T + R_l$ 
11     $K_l = P_l^- H_l^T S_l^{-1}$ 
12     $\bar{x}_l = \bar{x}_l^- + K_l (y_l - h_l(\bar{x}_l^-))$ 
13     $P_l = (I - K_l H_l) P_l^-$ 
14  end
15   $\hat{x}_k = \bar{x}_k$ 
16 end

```

The EOFIR filter requires a horizon length of N , this can be determined experimentally. The greater the value of N , the slow the estimate computation. The EOFIR Filter has a batch form [26], which is more quickly running on parallel computing. The value of N which minimizes the RMSE is known as N_{opt} .

3.3. Results

For the test environment, we deploy 7 anchors in fixed positions in a room of 6x5m approximately. We don't use any particular arrangement for the tags. They were positioned arbitrarily. The robot has an I2C digital compass S320160 to get its orientation. In our experiment, the robot always follows a tangent orientation to the trajectory. The precision of the compass is ± 4 deg. The path described by the TWOR is circular. The localization estimation is in figure 7. And the errors can be viewed in figure 8.

- In red, we can observe the result for the non-probabilistic method. Even without knowledge of the model, the LS estimator can recover the trajectory but with a large bias. The RMSE for this estimator was 0.1572 m.
- In magenta, the classical EKF algorithm was used assuming no errors due to fading. The estimation was better than in LS estimator. The RMSE was 0.0124
- In blue, the EKF filter with bias correction, the improvements over the previous localization algorithms are clear, the RMSE is 0.0091.

- Finally, in orange, the EOFIR algorithm with $N_{opt} = 8$, this is the best result with an RMSE of 0.0065.

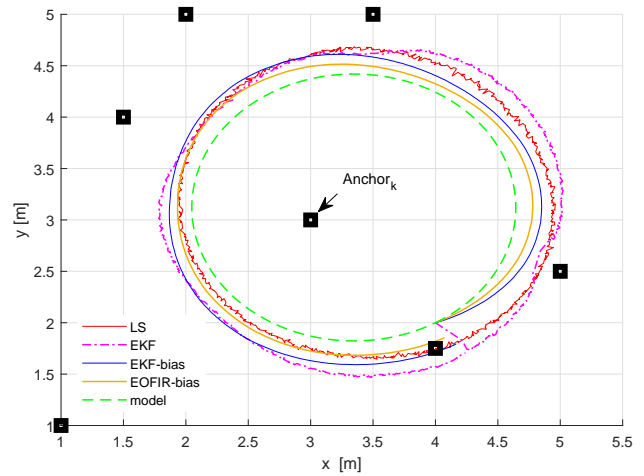


Fig. 7. Estimated position of TWOR

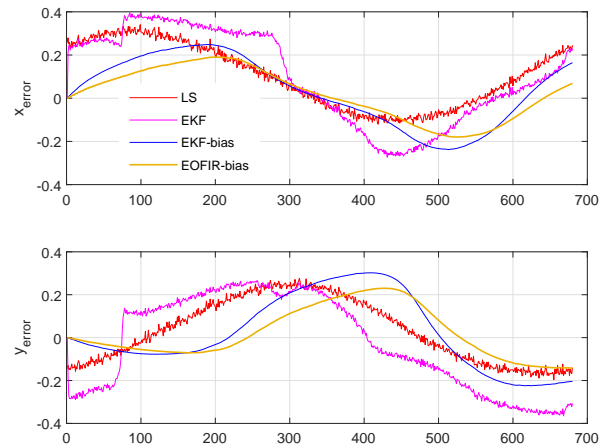


Fig. 8. Error obtained with the localization algorithms

4. Conclusions

In this paper, we develop an environment test for tracking a TWOR in UWB sensor network. Then, through a simple experiment, we determine the effects of fading in LOS conditions and propose a bias correction to the observation model. Finally, we perform a comparison between positioning algorithms considering unbiased/biased measurements. It should be noted that the EOFIR filter has better results than the EKF Filter, but in theory, both filters are equivalent. In a real scenario, each anchor is in different conditions (LOS, NLOS, and multipath), and the EOFIR filter has more robustness against disturbance than the EKF Filter. The first was always bounded and hence it is inherently stable. The second one was derived in IIR form, so it has a slow disturbance rejection.

References

- [1] A. S. Kundua, O. Mazumdera, P. K. Lenkab, S. Bhaumik, "Omnidirectional assistive wheelchair: Design and control with isometric myoelectric based intention classification," *Procedia Computer Science*, 2017, 105, 6874.
- [2] J. Moreno, E. Clotet, R. Lupiaez, M. Tresanchez, D. Martnez, T. Palleja, et al., "Design, implementation and validation of the three-wheel holonomic motion system of the assistant personal robot (APR)". *Sensors*, 2016, 16(10), 1658.
- [3] J. Qian, B. Zi, D. Wang, Y. Ma, D. Zhang, "The design and development of an omni-directional mobile robot oriented to an intelligent manufacturing system," *Sensors*, 2017,17(9), 2073.
- [4] Anand Singh Rajawat, Pradeep Bedi, S. B. Goyal, Piyush Kumar Shukla, Atef Zaguia, Aakriti Jain, Mohammad Monirujjaman Khan, "Reformist Framework for Improving Human Security for Mobile Robots in Industry 4.0", *Mobile Information Systems*, vol. 2021, Article ID 4744220, 10 pages, 2021. <https://doi.org/10.1155/2021/4744220>
- [5] G. I. R. K. Galgamuwa, L. K. G. Liyanage, M. P. B. Ekanayake and B. G. L. T. Samaranyake, "Simplified controller for three wheeled omni directional mobile robot," 2015 IEEE 10th International Conference on Industrial and Information Systems (ICIIS), 2015, pp. 314-319, doi: 10.1109/ICIINFS.2015.7399030.
- [6] T. Terakawa, M. Komori, K. Matsuda, "Motion Analysis of an Omnidirectional Mobile Robot with Wheels Connected by Passive Sliding Joints," In: Uhl, T. (eds) *Advances in Mechanism and Machine Science. IFToMM WC 2019. Mechanisms and Machine Science*, 2019, vol 73. Springer, Cham.
- [7] Luis Gracia, Josep Tornero,"A Practical Approach for Motion Planning of Wheeled Mobile Robots," In (Ed.), *Motion Planning*. IntechOpen, 2008, <https://doi.org/10.5772/6017>
- [8] S. Kallweit, R. Walenta, M. Gottschalk,"ROS Based Safety Concept for Collaborative Robots in Industrial Applications," In: Borangiu, T. (eds) *Advances in Robot Design and Intelligent Control. Advances in Intelligent Systems and Computing*, 2016, vol 371. Springer, Cham. https://doi.org/10.1007/978-3-319-21290-6_3
- [9] M. von Tschirschnitz, M. Wagner, M. O. Pahl and G. Carle, "Clock Error Analysis of Common Time of Flight based Positioning Methods," 2019 International Conference on Indoor Positioning and Indoor Navigation (IPIN), 2019, pp. 1-8, doi: 10.1109/IPIN.2019.8911772.
- [10] F.B. Sorbelli, C.M. Pinotti, G. Rigoni, "Range-free Localization Algorithms with Mobile Anchors at Different Altitudes: A Comparative Study," *ACM International Conference Proceeding Series*, 2020; Vol-F1656, pp. 883894.
- [11] N. Ayoobi, M. Ghavami, A. Rabiei, "A novel motion-model-free UWB short-range positioning method," *Signal, Image and Video Processing*, 2020, doi:14. 10.1007/s11760-019-01613-2.
- [12] Anton Ledergerber, Raffaello DAndrea, "Ultra-wideband range measurement model with Gaussian processes,"*IEEE Conference on Control Technology and Applications (CCTA)*,2017, doi:10.1109/ccta.2017.8062738
- [13] J. Youssef, B. Denis, C. Godin and S. Leseq, "Enhanced UWB Indoor Tracking through NLOS TOA Biases Estimation," *IEEE GLOBECOM 2008 - 2008 IEEE Global Telecommunications Conference*, 2008, pp. 1-5, doi: 10.1109/GLOCOM.2008.ECP.925.
- [14] A. Ledergerber and R. Dandrea, "Calibrating Away Inaccuracies in Ultra Wideband Range Measurements: A Maximum Likelihood Approach," in *IEEE Access*, vol. 6, pp. 78719-78730, 2018, doi: 10.1109/ACCESS.2018.2885195.
- [15] N. M. Senevirathna, O. De Silva, G. K. I. Mann and R. G. Gosine, "Kalman Filter based Range Estimation and Clock Synchronization for Ultra Wide Band Networks," 2020 IEEE/RSJ International Conference on Intelligent Robots and Systems (IROS), 2020, pp. 9027-9032, doi: 10.1109/IROS45743.2020.9340971.
- [16] Bas van der Heijden, Anton Ledergerber,Rajan Gill, Raffaello DAndrea, "Iterative Bias Estimation for an Ultra-Wideband Localization System," *IFAC-PapersOnLine*, 2020, Vol 53,pp. 1391-1396. 10.1016/j.ifacol.2020.12.1889.
- [17] K. Yu, K. Wen, Y. Li, S. Zhang and K. Zhang, "A Novel NLOS Mitigation Algorithm for UWB Localization in Harsh Indoor Environments," in *IEEE Transactions on Vehicular Technology*, vol. 68, no. 1, pp. 686-699, Jan. 2019, doi: 10.1109/TVT.2018.2883810.
- [18] T. Zhou, Y. Cheng, B. Lian and Y. Zhang, "Research on UWB Localization Based on TOA in Indoor NLOS Environment," 2018 9th International Conference on Information Technology in Medicine and Education (ITME), 2018, pp. 983-988, doi: 10.1109/ITME.2018.00219.
- [19] G. Campion, G.Bastin, B. DAndrea-Novel, "Structural properties and classification of kinematic and dynamic models of wheeled mobile robots," In *Proceedings of the 1993 IEEE International Conference on Robotics and Automation*, Atlanta, GA, USA, 26 May 1993, pp. 462469
- [20] A. Gfrerrer, "Geometry and kinematics of the Mecanum wheel,"*Computer Aided Geometric Design*, Volume 25, Issue 9, 2008,pp. 784-791
- [21] Y. Jiang and V. C. M. Leung, "An Asymmetric Double Sided Two-Way Ranging for Crystal Offset," 2007 International Symposium on Signals, Systems and Electronics, 2007, pp. 525-528, doi: 10.1109/ISSSE.2007.4294528.
- [22] D. Neirynek, E. Luk and M. McLaughlin, "An alternative double-sided two-way ranging method," 2016 13th Workshop on Positioning, Navigation and Communications (WPNC), 2016, pp. 1-4, doi: 10.1109/WPNC.2016.7822844.
- [23] Lian Sang C, Adams M, Hrmann T, Hesse M, Porrman M, Rückert U. "Numerical and Experimental Evaluation of Error Estimation for Two-Way Ranging Methods," *Sensors*. 2019; 19(3):616. <https://doi.org/10.3390/s19030616>
- [24] R. Zetik, M. Eschrich, S. Jovanoska and R. S. Thoma, "Looking behind a corner using multipath-exploiting UWB radar," in *IEEE Transactions on Aerospace and Electronic Systems*, vol. 51, no. 3, pp. 1916-1926, July 2015, doi: 10.1109/TAES.2015.140303.
- [25] Sidorenko Juri, Schatz Volker, Scherer-Negenborn Norbert, Arens Michael, Hugentobler Urs. "Decawave UWB Clock Drift Correction and Power Self-Calibration," *Sensors*, 2019, 19(13):2942, doi:10.3390/s19132942.
- [26] Shmaliy, Y., Zhao, S. (2022). *Optimal and robust state estimation: Finite Impulse Response (FIR) and Kalman approaches*. Wiley-IEEE Press.

Creative Commons Attribution License 4.0 (Attribution 4.0 International, CC BY 4.0)

This article is published under the terms of the Creative Commons Attribution License 4.0

https://creativecommons.org/licenses/by/4.0/deed.en_US